Original article

Pulmonary annular motion velocity reflects right ventricular outflow tract function in children with surgically repaired congenital heart disease

Yasunobu HAYABUCHI, MD, PhD; Akemi ONO, MD, Yukako HOMMA, MD, Shoji KAGAMI, MD, PhD

Department of Pediatrics, Tokushima University, Tokushima, Japan

Short title: Pulmonary annular motion velocity in repaired CHD

Address for correspondence: Yasunobu Hayabuchi, MD

Department of Pediatrics, Tokushima University

Kuramoto-cho 3, Tokushima 770-8305, Japan

Tel: +81-886-33-7135

Fax: +81-886-31-8697

E-mail: hayabuchi@tokushima-u.ac.jp

ABSTRACT

Right ventricular (RV) dysfunction is generally evaluated using analyses of tricuspid annular motion. However, it represents only one aspect of RV performance. Whether measuring pulmonary annular motion velocity could serve as a novel way to evaluate global RV and/or RV outflow tract (RVOT) performance in pediatric congenital heart disease (CHD) patients with surgically repaired RVOT was evaluated. In this prospective study, tissue Doppler-derived pulmonary annular motion velocity was measured in children (aged 2-5 years) with RVOT reconstruction (RVOTR group, n = 48) and age-matched healthy children (Control, n = 60). The types of RVOTR procedures were as follows: pulmonary valve-sparing procedure (PVS, n = 7); transannular patch with monocusp valve reconstruction (TAP, n = 29); and RV-to-PA conduit reconstruction using a pericardial valve with expanded polytetrafluoroethylene conduit (Rastelli, n = 12). Pulmonary annular motion velocity waveforms comprised systolic bimodal (s1' and s2') and diastolic e' and a' waves in all participants. The peak velocities of s1', s2', e', and a' were significantly lower in the RVOTR group than in the control group (all $p < 0.0001$). Furthermore, these parameters depended significantly on the type of surgical procedure. The peak velocities of s1', s2', and e' had significant correlations with RVOT ejection fraction (RVOT-EF) ($r = 0.56$, 0.49, and 0.34, respectively) and RVOT fractional shortening (RVOT-FS) ($r = 0.72$, 0.55, and 0.41, respectively), although there were no significant correlations between pulmonary annular motion and global RV function, including RV ejection fraction (RVEF) and RV fractional area change (RVFAC) in the assessment of all RVOTR group patients. The pulmonary annular motion parameters in the PVS group had significant correlations

with both global RV and RVOT performance. The TAP group showed significant correlations between RVOT function and pulmonary annular motion. The Rastelli group showed almost no significant correlations between RV/RVOT function and tissue Doppler parameters. Pulmonary annular motion velocity is a simple, rapid, reproducible, and useful method of assessing RVOT function in children with surgically repaired CHD.

Keywords: Right ventricular outflow tract, congenital heart disease, children, tissue Doppler imaging

INTRODUCTION

Accurate determination and serial follow-up of right ventricular (RV) function are important in the management of surgically repaired congenital heart disease (CHD) patients with RV outflow tract reconstruction (RVOTR), since RV dysfunction in these patients is associated with poor clinical outcomes [1]. However, the quantitative assessment of RV function remains challenging, mainly because of the complex RV geometry and the thin myocardial wall [2].

RV dysfunction is generally evaluated using analyses of longitudinal shortening, including tricuspid annular plane systolic excursion (TAPSE), tissue Doppler-derived tricuspid annular s' wave velocity, and longitudinal strain of the RV free wall in the apical four-chamber view [3]. However, RV morphology is complex, and some regions are not evaluable by analyses in only one direction. The shape of the RV is triangular when viewed from the front. Tricuspid annular motion velocity corresponds to only one of the three sides of the triangle. We hypothesized that pulmonary annular motion velocity would correspond to another side of the triangle and would reflect right ventricular outflow tract (RVOT) function. Although RVOT performance is reported to be important in RV ejection [4, 5], few previous investigations have focused on RVOT performance [6-8].

Therefore, the aim of this study was to determine the characteristics of pulmonary annulus velocity waveforms obtained using tissue Doppler imaging (TDI) and to determine whether tissue Doppler-derived pulmonary annular motion velocity can serve as a tool for global RV or regional RVOT functional assessment in pediatric CHD patients with a surgically reconstructed RVOT.

MATERIALS AND METHODS

Study design and population

This was a single-center, prospective, observational study. The study group included 48 consecutive postoperative CHD patients with RVOTR (RVOTR group; mean age, 3.6 ± 0.9 y; range, 2.0 – 5.0 y). Diagnoses included: tetralogy of Fallot (TOF, n = 34); ventricular septal defect with pulmonary atresia (VSD/PA, n = 9); and double outlet right ventricle (DORV, n = 5). The types of procedure were as follows: pulmonary valve-sparing procedure (PVS, n = 7); transannular patch with monocusp valve reconstruction (TAP, n = 29); and RV-to-PA conduit reconstruction using a pericardial valve with expanded polytetrafluoroethylene conduit (Rastelli, n = 12). Age at surgical repair was 1.3 ± 0.7 (0.7 – 3.4) years. Thirty-nine (81.3%) of the RVOTR group patients underwent a modified Blalock-Taussig shunt as palliation. The patients underwent cardiac catheterization for routine postoperative evaluation. Echocardiography was performed within three days of cardiac catheterization. Sixty-two age-matched healthy children were also enrolled (control group; age, 3.7 ± 0.8 y; age range, 2.0 – 5.0 y). Participants were included in this study only if they were between 2 and 5 years of age and had normal electrocardiographic and transthoracic echocardiographic results. Data collected between December 2011 and August 2015 were analyzed. All protocols were approved by the Institutional Review Board of Tokushima University Hospital and conformed to the ethical guidelines of the Declaration of Helsinki (1975). The parents of all subjects provided their written, informed consent for their children to participate in the study.

Echocardiographic study

Standard and pulsed Doppler tissue echocardiography was performed using a Preirus digital ultrasound system (Hitachi-Aloka Medical Co., Tokyo, Japan) equipped with 1 – 5 and 3 – 7 MHz sector transducers. All Doppler data were acquired from subjects in the left lateral decubitus position during shallow respiration or end-expiratory apnea. Pulmonary annular motion velocity was measured using TDI in the long-axis view of the RVOT. Guided by the two-dimensional images, a sample volume with a fixed length of 5.0 mm was placed on the pulmonary annulus of the RV free wall side (Fig. 1A). The ultrasound beam was positioned parallel to the direction of pulmonary annular motion. Figures 1b and c show the pulmonary annular motion velocity curve in a normal subject and a patient with surgically repaired TOF, respectively. All tissue Doppler parameters were measured during three consecutive heart cycles by a single physician who was blinded to the patients' conditions, and mean values were calculated.

In addition to pulsed TDI, right ventricular fractional area change (RVFAC) was measured from the four-chamber view with a focus on the RV. The RV area (endocardial borders excluding trabeculae and papillary muscles) was measured at the end of diastole and at the end of systole. RVFAC was calculated using the formula: RVFAC (%) = 100 × (diastolic RV area - systolic RV area)/diastolic RV area. RVOT fractional shortening (RVOT-FS) was measured from the parasternal short-axis view using the M-mode images, as reported by Lindqvist et al [6]. RVOT-FS was calculated as follows: RVOT-FS (%) = 100 × (RVOT diastolic diameter - RVOT systolic diameter)/RVOT diastolic diameter. Imaging was performed at the level of the aortic

valve at maximal RVOT diameter, with the ultrasound beam perpendicular to the RVOT walls, after optimization of focus, compression, and gain settings (Fig. 1d). Furthermore, participants were assessed by conventional, two-dimensional, M-mode, pulsed, continuous, and color Doppler echocardiography. Transmitral and transtricuspid diastolic blood flow velocities were determined in the apical 4-chamber view by placing the pulsed Doppler sample volume at the tip of the valve leaflets. Tissue Doppler velocities of the mitral annulus and the tricuspid annulus (e', a', and s') were also evaluated from the apical four-chamber view. The left ventricular ejection fraction (LVEF) was calculated from apical two-chamber and four-chamber images using the biplane Simpson's technique. All parameters were measured during three cardiac cycles and then averaged.

Cardiac catheterization

All patients underwent cardiac catheterization within three days of echocardiography. Catheterization and angiography using an Integris Allura 9 Biplane (Phillips Medical Systems, Best, The Netherlands) were performed with 4 to 6-Fr catheters. All patients were intubated and examined by biplane anteroposterior and lateral projection angiography. Ventricular volume was assessed by means of ventriculography and calculated using the area-length method for the left ventricle and Simpson's rule for the RV using quantitative CAW2000 cardiac analysis software (ELK Corporation, Osaka, Japan). Furthermore, the segmental analysis of the RV is displayed in Figures 1e and f. After manual tracing of the endocardial borders of the full RV volume, three anatomic landmarks (tricuspid annulus border, pulmonary annulus border, and apex) were identified. On the basis of these anatomic landmarks defined by the

observer, two surface landmarks were subsequently identified mathematically. Landmark A was defined as the region at 50% of the distance between the pulmonary annulus border and the apex. Landmark B was defined as the region at 50% of the distance between the tricuspid annulus border and the pulmonary annulus border. From these surface landmarks, the RVOT component was identified. Subsequently, the software provided volume computations, from which RVOT end-diastolic volume (RVOT-EDV), RVOT end-systolic volume (RVOT-ESV), and RVOT ejection fraction (RVOT-EF) were evaluated.

Statistical analysis

All data are expressed as means ± standard deviation (SD) or as medians with 5^{th} – 95^{th} percentiles. Statistical significance was determined using Student's *t*-test, Mann-Whitney's *U*-test, or the Kruskal-Wallis test followed by Dunn's test, as appropriate. Linear regression analyses were performed for correlations between the pulmonary annular motion velocity and hemodynamic parameters, and Pearson's or Spearman's correlation coefficients were calculated, as appropriate. All statistical data were calculated using Prism version 6.0 (GraphPad Software, San Diego, CA, USA) installed on a desktop computer. A value of $p < 0.05$ (two-sided) was considered significant. Intra-observer and inter-observer reproducibilities of TDI measurements were assessed using Bland-Altman analysis in a blinded manner. Data were recorded and assessed at five-minute intervals by observers 1 and 2 from 20 randomly selected participants (RVOTR, n = 10; controls, n = 10). For intra-observer variability, data were analyzed twice, 8 weeks apart. Inter-observer variability was assessed by analyzing data from two separate observers blinded to each other's results.

RESULTS

Patient characteristics

Of the 62 healthy children, one with arrhythmia and one with a small atrial septal defect were excluded. No patients in the RVOTR group were excluded from the subsequent analyses. Accordingly, the study group included 60 healthy children (mean age, 3.7 ± 0.8 y; range, 2.0-5.0 y) and 48 with postoperative CHD with RVOTR (mean age, 3.6 ± 0.9 y; range, 2.0-5.0 y).

Table 1 shows the clinical, echocardiographic, and hemodynamic data of the participants. Age, height, weight, body surface area (BSA), and heart rate (HR) did not differ significantly between the RVOTR group and controls. QRS duration was significantly longer in the RVOTR group. Left ventricular end-diastolic dimension (LVEDD), LVFS, and LVEF were not significantly different, whereas RVFAC and RVOT-FS were significantly lower in the RVOTR group than in the control group. Since the control group did not undergo cardiac catheterization, the hemodynamic data obtained from the invasive examination of the RVOTR group could not be compared between the groups.

Figure 1 shows a representative example of the color TDI and profile of the pulmonary annular motion velocity in a healthy child and a patient in the RVOTR group. The region of interest was positioned on the RV free wall side of the pulmonary annulus, as indicated by the arrow. Figure 1b shows the pulmonary annular motion velocity curve in a normal subject. The systolic wave showed a bimodal waveform (s1’ and s2’ waves). The e’ and a’ waves in diastole were shown to be the same as the mitral and tricuspid annular motions. Figure 1c shows representative recordings of the pulmonary

annular motion velocity waveforms in a surgically repaired CHD patient with RVOTR. Although the peak velocity of each wave was low, the systolic bimodal waveform and diastolic e' and a' waves were demonstrated to be the same as in normal subjects. Figure 2a-d compares the peak velocity of each wave between the two groups. The peak velocities of s1', s2', e', and a' in the RVOTR group were 5.8 ± 2.0, 3.4 ± 1.3, 8.6 ± 3.3, and 3.2 ± 1.2 cm/s, respectively, all of which were significantly lower than those of the control group (11.6 ± 2.0, 4.8 ± 1.3, 12.3 ± 2.2, and 4.9 ± 1.8 cm/s, respectively; all $p < 0.0001$). Furthermore, the difference in peak velocity was assessed depending on the type of surgical procedure (Fig. 2e-h). The s1' was significantly lower in the TAP group than in the PVS group (5.9 ± 1.7 vs 8.4 ± 1.6 cm/s; $p < 0.05$). The peak velocity of s1' in the Rastelli group was 4.1 ± 1.1 cm/s, significantly lower than in the PVS and TAP groups ($p < 0.0001$ and < 0.05, respectively). The peak velocity of s2' was significantly lower in the TAP and Rastelli groups than in the PVS group (3.4 ± 1.2, 2.6 ± 0.5, and 4.9 ± 1.5 cm/s; $p < 0.05$ and < 0.005, respectively), whereas there was no significant difference between the TAP and Rastelli groups. The Rastelli group had significantly lower peak velocity of e' than the PVS group (6.2 ± 2.1 vs 10.9 ± 2.8 cm/s; $p < 0.001$). The e' of the TAP group was 8.8 ± 3.3 cm/s and showed no significant difference from the values of the PVS or TAP groups. There was no significant difference in the peak velocity of the a' wave among the PVS, TAP, and Rastelli groups (3.9 ± 1.9, 3.3 ± 1.0, and 2.6 ± 0.9 cm/s, respectively).

Correlations between TDI-derived pulmonary annular motion and RV/RVOT function

Next, the correlations between the parameters obtained from TDI-derived pulmonary annular motion and global RV performance in the RVOTR group were

assessed. Global RV function was assessed by RVEF and RVFAC. Figure 3a-d demonstrates the relationship between pulmonary annular motion velocity and RVEF. The peak velocity of each wave had no significant correlation with RVEF. In regard to the correlation with RVFAC (Fig. 3e-h), there was no significant correlation for each wave. Next, the correlations between the TDI-derived pulmonary annular motion and RVOT performance were assessed. Figure 4a-d shows the correlation between the RVOT-EF evaluated by right ventriculography and pulmonary annular motion velocity. The peak velocities of s1', s2', and e' had significant correlations with RVOT-EF ($r = 0.56$, 0.49, and 0.34, $p < 0.0001$, < 0.0005, and < 0.05, respectively). RVOT-FS also had significant correlations with the peak velocities of s1', s2', and e' ($r = 0.72$, 0.55, and 0.41; $p < 0.0001$, < 0.0001, and < 0.005 respectively) (Fig. 4E-H).

Furthermore, the correlations between tissue Doppler-derived pulmonary annular motion parameters and RV and RVOT function were investigated in each of the 3 groups based on the type of RVOT reconstruction. Fig. 5 shows the relationships in the PVS group. RVFAC had significant correlations with the peak velocities of s1', e', and a' ($r = 0.76$, 0.82, and 0.83, respectively; all $p < 0.05$). The peak velocities of s1' also had significant correlations with RVOT-EF and RVOT-FS ($r = 0.79$ and 0.84, respectively; both $p < 0.05$). The correlations between pulmonary annular motion and RV/RVOT performance in the TAP group are shown in Fig. 6. RVFAC had a significant correlation with the peak velocity of a' ($r = 0.38$, $p < 0.05$). The peak velocities of s1'and s2' had significant correlations with RVOT-EF ($r = 0.49$ and 0.39, $p < 0.005$ and < 0.05, respectively) and with RVOT-FS ($r = 0.76$ and 0.48, $p < 0.0001$ and < 0.001, respectively). Fig. 7 shows the relationships in the Rastelli group. RVEF was significantly correlated with s1' ($r = 0.77$, $p < 0.01$).

Reproducibility

The inter- and intra-observer reproducibilities of the TDI analysis of pulmonary annular motion were determined by Bland-Altman analysis of 20 randomly selected participants (RVOTR, n = 10; control, n = 10). Figure 5 shows Bland-Altman plots for intra-observer and inter-observer variabilities (bias ± 2 SDs [95% limit of agreement]), respectively. They showed minimal bias and substantial agreement.

DISCUSSION

The present results showed that tissue Doppler-derived pulmonary annular motion velocities of s1', s2', and e' waves significantly reflected RVOT performance in patients with surgically repaired CHD. Pulmonary annular motion velocity was demonstrated to be a simple, rapid, reproducible, and highly characteristic method for evaluating RVOT function. The differences in parameters between healthy controls and the RVOTR group were obvious. Furthermore, the peak velocities of the s1', s2', and e' waves had significant correlations with RVOT performance, indicated by RVOT-FS and RVOT-EF.

To the best of our knowledge, our previous study is the first application of pulmonary annular motion velocity obtained by TDI as a tool for RVOT functional assessment [9]. However, it did not determine whether pulmonary annular motion could serve as an important guideline for assessing quantitative global RV or RVOT function. The present study demonstrated that pulmonary annular motion indicates RVOT

performance, but not overall RV performance, in patients with surgically repaired CHD. Analyzing the relationships between TDI parameters and RV/RVOT function based on the type of RVOT reconstruction, the correlations in the PVS and TAP groups were relatively meaningful, whereas the correlations in the Rastelli group were quite low. This would be because RVOT wall motion is extremely limited by the prosthetic materials, which affect the TDI parameters and RVOT performance. The PVS group showed significant correlations between RV global/RVOT function and some pulmonary annular motion parameters. The TAP group showed significant correlations between pulmonary annular motion and RVOT function, but not with global RV function. These are reasonable results, because the function of the RVOT and global RV can be more closely related in the PVS group than in the TAP group.

Assessment of RV function in various cardiac diseases is important but challenging due to the complex anatomy and geometry of the RV, for which few functional evaluations are available. Patients with a repaired RVOT require lifelong follow-up that includes serial assessment of RV and RVOT function. Therefore, the TDI-derived pulmonary annular motion velocity can be a novel, promising method of assessing serial RVOT function in children with repaired CHD.

Current quantitative methods such as two-dimensional fractional area change (FAC), TAPSE, tricuspid s' wave of TDI, and 3-dimensional (3D) echocardiography all have limitations [3]; FAC does not necessarily represent the ejection fraction of the entire RV, and TAPSE and tricuspid s' measure only longitudinal displacement of the lateral RV wall. Three-dimensional echocardiography is limited by the current imaging quality of the RV borders [2, 10]. Because the accuracy of quantitative assessment of RV function by two-dimensional echocardiography is hampered by the chamber's

complex geometry [2, 10], nongeometric methods to assess RV myocardial motion and deformation have been explored. One such method, TDI, allows the quantitative assessment of longitudinal RV function on the basis of myocardial velocity estimation at the level of the tricuspid valve annulus [11, 12]. Although several studies have examined the utility of RV free wall TDI in surgically repaired TOF [13-15], these investigations have not addressed the potentially confounding effect of RVOT dysfunction on myocardial velocities at the base of the RV.

Patients with surgically repaired TOF have impaired systolic function of the RVOT [14]. Determination of the pulmonary annular motion velocity can be useful to evaluate RVOT performance in these patients. Myocardial damage induced by cardiac surgery and RVOT reconstruction might have negative effects on these parameters [4, 16]. Furthermore, the pressure-loaded RV induced by RVOT stenosis, pulmonary stenosis, or pulmonary hypertension might affect RVOT function and pulmonary annular motion velocity. Contractions of the RVOT and RV body are important determinants of global RV systolic function in surgically repaired CHD patients. Greutmann et al. found that severely decreased RVOT systolic function in TOF patients with a surgically reconstructed RVOT can be compensated for by increased radial and transverse shortening of the RV body [16]. Their result also supports our proposal that pulmonary annular motion velocity might be worth measuring in all patients with a reconstructed RVOT. While the function of the inflow and outflow components of the RV can be closely related in the normal heart [17], this relationship would be weak and unpredictable in patients with a surgically repaired RVOT [18, 19]. The present study also showed that there was no correlation between the pulmonary annular motion velocity and global RV function. Kutty et al. showed that the correlation between

TDI-measured tricuspid annular s' and global RV function is acceptable in patients with repaired TOF with mild or less RVOT dysfunction, but it is weak in those with moderate or greater RVOT dysfunction [4]. Their findings are compatible with the data of the present study. In patients with RVOT reconstruction, a functional discrepancy is present between the outflow tract and the inflow tract. From this perspective, it would be more useful to evaluate pulmonary annular motion to assess RVOT in these patients with repaired RVOT.

The present results suggest that measuring pulmonary annular motion provides additional information about what is normal function for the healthy pediatric RVOT. Furthermore, together with the established longitudinal RV functional parameters TAPSE and s', it would provide detailed assessment of RVOT performance in children with cardiac diseases. Since the impairment of RVOT performance would occur prior to global RV functional decline, the assessment of RVOT performance using TDI parameters can be clinically very useful and important for long-term follow-up. The changes in RV/RVOT function and pulmonary annular motion over time should be evaluated in a future study.

Limitations

The sample cohort was relatively small, but TDI parameters were compared between the RVOTR group and age-matched healthy individuals, and distinctive waveforms and significantly different peak velocities were found. Some degree of angulation between the Doppler beam and the true direction of myocardial movement may exist. Although such angulation may be small, the data presented herein are for velocity along the direction of the Doppler beam and might not indicate actual

myocardial velocity. Moreover, because pulsed TDI is limited by a stationary sample volume being positioned on a moving target, the effect of translation is not removed. Furthermore, the motion of the RV free wall might be restricted due to postoperative adhesions in patients with surgically corrected CHD. Such RV adhesions to the chest wall would affect postoperative pulmonary annular motions measured using TDI. In addition, the artificial material might have a major impact on the tissue Doppler imaging data. In the present study, the correlations between TDI parameters and RV/RVOT performance were weak in the Rastelli group compared with the PAS and TAP groups.

It is expected that many factors affect the TDI-derived parameters in surgically repaired CHD patients. The age of operation, cross-clamp time, conduction disturbances, residual abnormalities, including pulmonary insufficiency, RV dilation, and peripheral pulmonic stenosis might influence the results of the myocardial velocities. In the present study, how these affect pulmonary annular motion was not assessed. Future studies are needed to elucidate these effects.

In the present investigation, the relationship between pulmonary annular motion and RV performance obtained by cardiac catheterization for postoperative evaluation was evaluated. Although cardiac magnetic resonance imaging (CMR) represents the current gold standard of cardiac function, current acquisition techniques are susceptible to error and artifacts when performed in children because of their higher heart rates, higher prevalence of sinus arrhythmia, and inability to breath-hold. In the present study, there were difficulties in the method of RV segmentation. The determination of the RVOT portion using two landmark points is relatively problematic. A previous study reported that CMR can be quite useful to evaluate RVOT performance

[4]. The septal and parietal bands were used as markers for the boundary between the RV sinus and RVOT in this study. However, it is extremely difficult to evaluate RVOT volume with the same method by right ventriculography. Future studies are needed to evaluate the correlation between tissue Doppler imaging and CMR.

Lastly, pulmonary annular motion may be an echocardiographic parameter of RVOT function, not an estimate of global RV function. Thus, the study did not suggest that the pulmonary annular motion velocity can be an alternative index to global RV function. We did not intend to indicate the superiority of this method over TAPSE, tricuspid annular s' wave velocity, and longitudinal strain of the RV free wall. Further studies are needed to determine whether pulmonary annular motion could serve as an important guideline for assessing RVOT function and to predict prognosis and response to therapy.

Conclusions

Pulmonary annular velocity is a promising echocardiographic tool for evaluating RVOT function in patients with surgically repaired CHD.

Conflict of interest: The authors declare that they have no conflict of interest.

Ethical approval: All procedures performed in studies involving human participants were in accordance with the ethical standards of the institutional and/or national research committee and with the 1964 Helsinki declaration and its later amendments or comparable ethical standards.

Informed consent: Informed consent was obtained from all individual participants' parents included in the study.

REFERENCES

1. Gatzoulis MA, Balaji S, Webber SA, Siu SC, Hokanson JS, Poile C, Rosenthal M, Nakazawa M, Moller JH, Gillette PC, Webb GD, Redington AN (2000) Risk factors for arrhythmia and sudden cardiac death late after repair of tetralogy of Fallot: a multicentre study. Lancet 356(9234):975-981

2. Lai WW, Gauvreau K, Rivera ES, Saleeb S, Powell AJ, Geva T (2008) Accuracy of guideline recommendations for two-dimensional quantification of the right ventricle by echocardiography. Int J Cardiovasc Imaging 24(7):691-698

3. Rudski LG, Lai WW, Afilalo J, Hua L, Handschumacher MD, Chandrasekaran K, Solomon SD, Louie EK, Schiller NB (2010) Guidelines for the echocardiographic assessment of the right heart in adults: a report from the American Society of Echocardiography endorsed by the European Association of Echocardiography, a registered branch of the European Society of Cardiology, and the Canadian Society of Echocardiography. J Am Soc Echocardiogr 23(7):685-713

4. Kutty S, Zhou J, Gauvreau K, Trincado C, Powell AJ, Geva T (2011) Regional dysfunction of the right ventricular outflow tract reduces the accuracy of Doppler tissue imaging assessment of global right ventricular systolic function in patients with repaired tetralogy of Fallot. J Am Soc Echocardiogr 24(6):637-643

5. Asmer I, Adawi S, Ganaeem M, Shehadeh J, Shiran A (2012) Right ventricular outflow tract systolic excursion: a novel echocardiographic parameter of right ventricular function. Eur Heart J Cardiovasc Imaging 13(10):871-877

6. Lindqvist P, Henein M, Kazzam E (2003) Right ventricular outflow-tract fractional shortening: an applicable measure of right ventricular systolic function. Eur J Echocardiogr 4(1):29-35

7. Koestenberger M, Ravekes W, Nagel B, Avian A, Heinzl B, Cvirn G, Fritsch P, Fandl A, Rehak T, Gamillscheg A (2014) Reference values of the right ventricular outflow tract systolic excursion in 711 healthy children and calculation of z-score values. Eur Heart J Cardiovasc Imaging 15(9):980-986

8. Koestenberger M1, Avian A, Ravekes W (2013) Reference values of the right ventricular outflow tract (RVOT) proximal diameter in 665 healthy children and calculation of Z-score values. Int J Cardiol 169(6):e99-101

9. Hayabuchi Y, Ono A, Kagami S (2016) Pulmonary annular motion velocity assessed using Doppler tissue imaging - Novel echocardiographic evaluation of right ventricular outflow tract function. Circ J 80(1):168-176

10. Wang J, Prakasa K, Bomma C, Tandri H, Dalal D, James C, James C, Tichnell C, Corretti M, Bluemke D, Calkins H, Abraham TP (2007) Comparison of novel echocardiographic parameters of right ventricular function with ejection fraction by cardiac magnetic resonance. J Am Soc Echocardiogr 20(9):1058-1064

11. Kukulski T, Hubbert L, Arnold M, Wranne B, Hatle L, Sutherland GR (2000) Normal regional right ventricular function and its change with age: a Doppler myocardial imaging study. J Am Soc Echocardiogr 13(3):194-204

12. Meluzin J, Spinarova L, Bakala J, Toman J, Krejcí J, Hude P, Kára T, Soucek M (2001) Pulsed Doppler tissue imaging of the velocity of tricuspid annular systolic motion; a new, rapid, and non-invasive method of evaluating right ventricular systolic function. Eur Heart J 22(4):340-348

13. Brili S, Alexopoulos N, Latsios G, Aggeli C, Barbetseas J, Pitsavos C, Vyssoulis G, Stefanadis C (2005) Tissue Doppler imaging and brain natriuretic peptide levels in adults with repaired tetralogy of Fallot. J Am Soc Echocardiogr 18(11):1149-1154

14. D'Andrea A, Caso P, Sarubbi B, Russo MG, Ascione L, Scherillo M, Cobrufo M, Calabrò R (2004) Right ventricular myocardial dysfunction in adult patients late after repair of tetralogy of Fallot. Int J Cardiol 94(2-3):213-220

15. Apostolopoulou SC, Laskari CV, Tsoutsinos A, Rammos S (2007) Doppler tissue imaging evaluation of right ventricular function at rest and during dobutamine infusion in patients after repair of tetralogy of Fallot. *Int J Cardiovasc Imaging* 23(1):25-31

16. Greutmann M, Tobler D, Biaggi P, Mah ML, Crean A, Wald RM, Silversides CK, Oechslin EN (2012) Echocardiography for assessment of regional and global right ventricular systolic function in adults with repaired tetralogy of Fallot. *Int J Cardiol* 157(1):53-58

17. Lytrivi ID, Ko HH, Srivastava S, Norton K, Goldman J, Parness IA, Lai WW, Nielsen JC (2004) Regional differences in right ventricular systolic function as

determined by cine magnetic resonance imaging after infundibulotomy. Am J Cardiol 94(7):970-973

18. Bodhey NK, Beerbaum P, Sarikouch S, Kropf S, Lange P, Berger F, Anderson RH, Kuehne T (2008) Functional analysis of the components of the right ventricle in the setting of tetralogy of Fallot. Circ Cardiovasc Imaging 1(2):141-147

19. Wald RM, Haber I, Wald R, Valente AM, Powell AJ, Geva T (2009) Effects of regional dysfunction and late gadolinium enhancement on global right ventricular function and exercise capacity in patients with repaired tetralogy of Fallot. *Circulation* 119(10):1370-1377

FIGURE LEGENDS

Figure 1. Representative recording of pulmonary annular motion evaluated by tissue Doppler imaging and assessment of right ventricular outflow tract function.

Long-axis view of the RVOT is shown, and the sample volume is positioned on the pulmonary annulus, as indicated by the arrow (a). Pulmonary annular motion velocity is determined in a healthy four-year-old boy (b) and a four-year-old girl with surgically repaired tetralogy of Fallot (c). The tissue Doppler-derived pulmonary annular motion velocity waveform comprises s1', s2', e', and a'. Right ventricular outflow tract fractional shortening (RVOT-FS) measurement using M-mode echocardiography from the parasternal short-axis view at the level of the aortic valve. Representative recordings from a four-year-old boy in the control group are shown (d). The measured RVOT-FS value is 61.1% in this case. Right ventriculography from a three-year-old girl in the TOF group in the anteroposterior (c) and lateral projections (d). The tricuspid annulus border, pulmonary annulus border, and apex are identified after tracing the endocardial border. On the basis of these landmarks, two surface landmarks (shown as A and B) are subsequently identified. Landmark A is defined as the region at 50% of the distance between the pulmonary annulus border and the apex. Landmark B is defined as the region at 50% of the distance between the tricuspid annulus border and the pulmonary annulus border. From these landmarks, the RVOT component is identified, and the RVOT ejection fraction (RVOT-EF) is calculated.

Ao, aorta; PA, pulmonary artery; RV, right ventricle, RVOT, right ventricular outflow tract; RVOTd, RVOT diastolic diameter; RVOTs, RVOT systolic diameter

Figure 2. Tissue Doppler-derived pulmonary annular motion velocity in the control group and in the congenital heart disease patients with right ventricular outflow tract reconstruction

The peak velocities of each wave obtained from the pulmonary annular motion velocity were compared between the control and right ventricular outflow tract reconstruction (RVOTR) groups (a – d). Furthermore, the patients in the RVOTR group were divided into 3 groups: pulmonary valve-sparing (PVS) repair group; transannular patch (TAP) reconstruction group; and the Rastelli procedure group. Pulmonary annular motion velocity was compared among these 3 groups. The boxes describe the distribution of peak velocity (25th and 75th percentiles; central line, median). The vertical lines represent the range between the 5th and 95th percentiles.

* $p < 0.0001$ vs control group, † $p < 0.05$ vs PVS group, ‡ $p < 0.0001$ vs PVS group, § $p < 0.05$ vs TAP group, ¶ $p < 0.005$ vs PVS group, # $p < 0.001$ vs PVS group

Figure 3. Correlations between the parameters obtained from tissue Doppler-derived pulmonary annular motion and global RV performance in patients with right ventricular outflow tract reconstruction

Relationships between RVEF and the pulmonary annular motion velocity (a-d) are shown. There are no significant correlations between RVEF and the peak velocity of each wave and between RVFAC and the peak velocity of each wave (e-h).

Figure 4. Correlations between the parameters obtained from tissue Doppler-derived pulmonary annular motion and RVOT performance in patients with right ventricular outflow tract reconstruction

There are significant correlations between RVOT-EF and the peak velocities of the s1' (a), s2' (b), and e' (c) waves, whereas there is no significant correlation with the a' wave (d). Furthermore, RVOT-FS is significantly correlated with the peak velocities of the s1' (e), s2' (f), and e' (g) waves. There is no significant correlation with the a' wave (h). Linear regression lines with the 95% confidence interval (dashed lines) are indicated.

Figure 5. Correlations between the parameters obtained from tissue Doppler-derived pulmonary annular motion and RV performance in patients with a pulmonary valve-sparing procedure (PVS group)

Figure 6. Correlations between the parameters obtained from tissue Doppler-derived pulmonary annular motion and RV performance in patients with transannular patch reconstruction (TAP group)

Figure 7. Correlations between the parameters obtained from tissue Doppler-derived pulmonary annular motion and RV performance in patients with the Rastelli procedure (Rastelli group)

Figure 8. Bland-Altman plots of intra-observer differences for peak velocities of the s1' (a), s2' (b), e' (c) and a' (d) waves, and inter-observer differences for peak velocities of the s1' (Ee), s2' (f), e' (g) and a' (h) waves

The solid and dotted lines show the mean difference and 95% limits of agreement, respectively.

Table 1

Table 1. Clinical characteristics of the subjects

		Control (n = 60)	RVOTR (n = 48)	p
Sex (male/female)		32/28	28/20	n.s.
Age (y)		3.7 ± 0.8	3.6 ± 0.9	n.s.
Weight (kg)		14.0 ± 4.3	13.3 ± 4.1	n.s.
Height (cm)		97.1 ± 6.1	92.7 ± 5.1	n.s.
Body surface area (m^2)		0.60 ± 0.08	0.57 ± 0.08	n.s.
Heart rate (bpm)		79 ± 12	84 ± 14	n.s.
QRS duration (msec)		87 ± 6	108 ± 14	< 0.0001
LVEDD (mm)		31.8 ± 2.4	30.2 ± 3.9	n.s.
LVFS (%)		36.6 ± 5.9	38.7 ± 6.1	n.s.
LVEF (%)		66.4 ± 5.6	66.3 ± 6.2	n.s.
Qp/Qs		-	1.02 ± 0.04	-
RVEDV (% of normal)		-	134 ± 18	-
RVEDP (mmHg)		-	8.2 ± 2.9	-
RVEF (%)		-	51.0 ± 9.2	-
RVOT-EF (%)		-	27.8 ± 9.4	-
RVSP (mmHg)		-	48.6 ± 17.6	-
mPAP (mmHg)		-	15.3 ± 4.1	-
RVFAC		47.8 ± 5.9	37.0 ± 8.3	< 0.0001
RVOT-FS		53.0 ± 7.7	28.3 ± 8.7	< 0.0001
Transmitral flow (m/sec)	E	1.05 ± 0.18	1.08 ± 0.19	n.s.
	A	0.44 ± 0.07	0.51 ± 0.17	< 0.005
Transtricuspid flow (m/sec)	E	0.54 ± 0.09	0.79 ± 0.18	< 0.0001
	A	0.29 ± 0.09	0.41 ± 0.13	< 0.0001
Mitral annular motion (cm/sec)	s’	9.9 ± 1.6	7.7 ± 1.7	< 0.0001
	e’	15.6 ± 2.9	13.7 ± 2.9	< 0.001
	a’	6.0 ± 1.3	5.1 ± 1.4	< 0.001
Tricuspid annular motion (cm/sec)	s’	13.5 ± 2.2	7.6 ± 1.8	< 0.0001
	e’	14.2 ± 2.3	10.5 ± 3.2	< 0.0001
	a’	8.6 ± 2.3	5.5 ± 2.1	< 0.0001

LVEDD, left ventricular end-diastolic dimension; LVEF, left ventricular ejection fraction; LVFS, left ventricular fractional shortening; mPAP, mean pulmonary arterial pressure; Qp/Qs, pulmonary to systemic blood flow ratio; RVEDP, right ventricular end-diastolic pressure; RVEDV, right ventricular end-diastolic volume; RVEF, right ventricular ejection fraction; RVFAC, right ventricular fractional area change; RVOT-EF, right ventricular outflow tract ejection fraction; RVOT-FS, right

ventricular outflow tract fractional shortening; RVOTR, right ventricular outflow tract reconstruction; RVSP, right ventricular systolic pressure; n.s., not significant

Figure 1

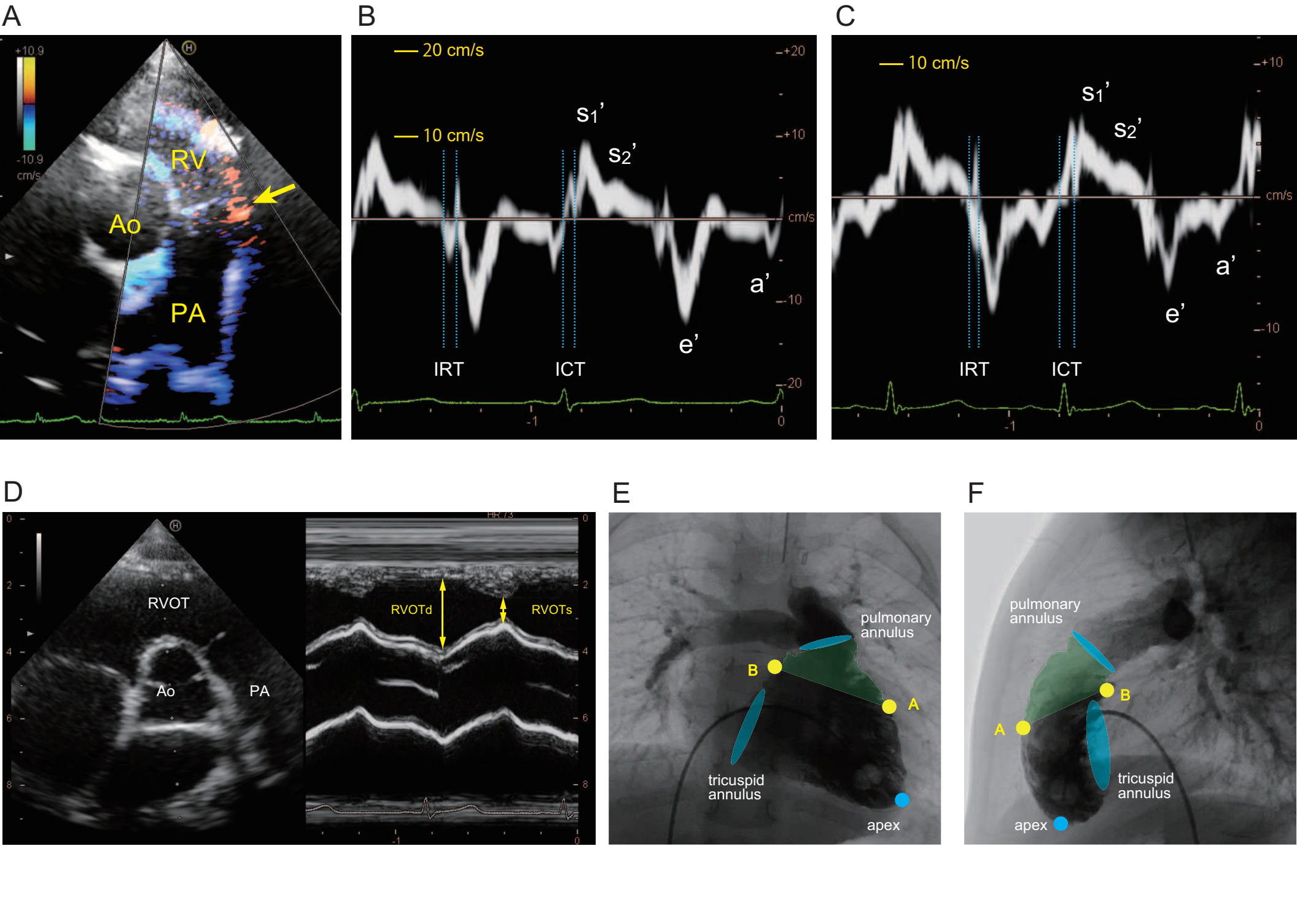
A
B
C
RV
Ao
PA
20 cm/s
10 cm/s
s1'
s2'
a'
e'
IRT
ICT
cm/s
10 cm/s
D
E
F
RVOT
Ao
PA
RVOTd
RVOTs
pulmonary annulus
tricuspid annulus
apex
A
B

Figure 2

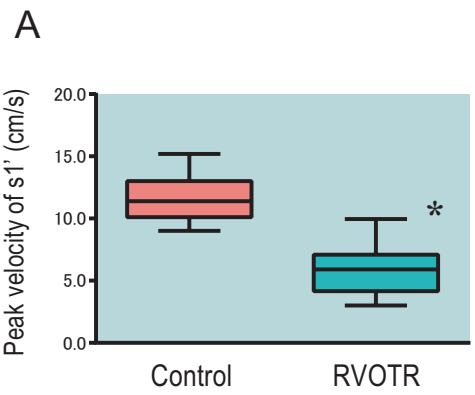
A
Peak velocity of s1' (cm/s)
20.0
15.0
10.0
5.0
0.0
*
Control
RVOTR

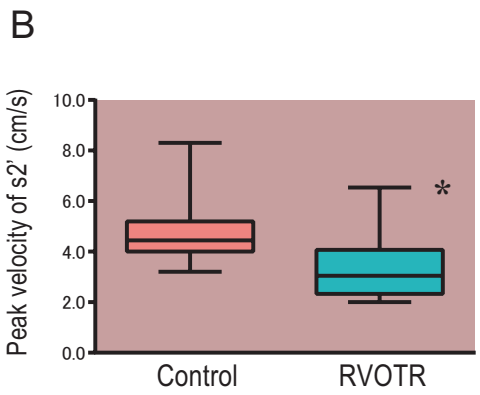
B
Peak velocity of s2' (cm/s)
10.0
8.0
6.0
4.0
2.0
0.0
*
Control
RVOTR

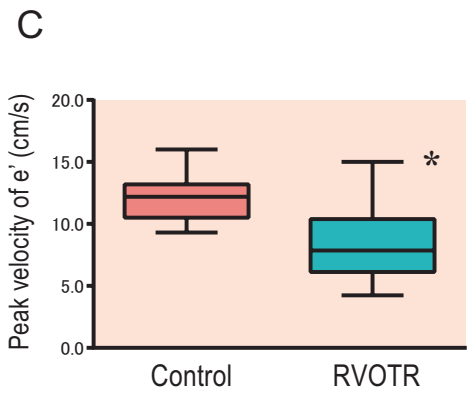
C
Peak velocity of e' (cm/s)
20.0
15.0
10.0
5.0
0.0
*
Control
RVOTR

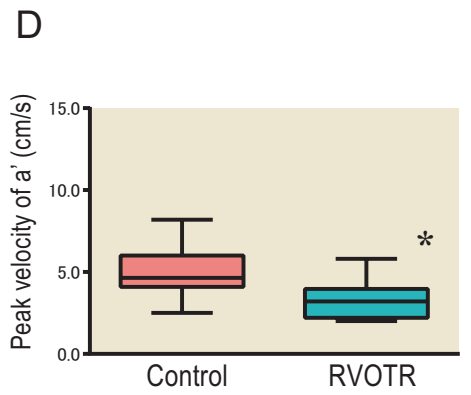
D
Peak velocity of a' (cm/s)
15.0
10.0
5.0
0.0
*
Control
RVOTR

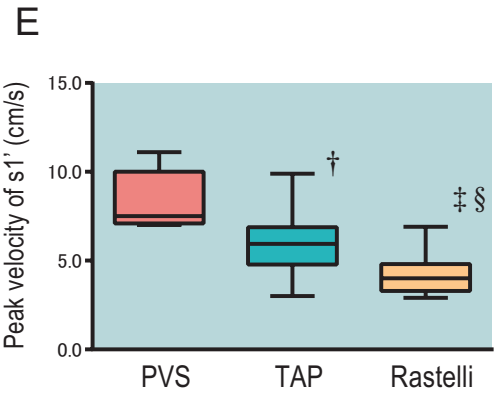
E
Peak velocity of s1' (cm/s)
15.0
10.0
5.0
0.0
†
‡ §
PVS
TAP
Rastelli

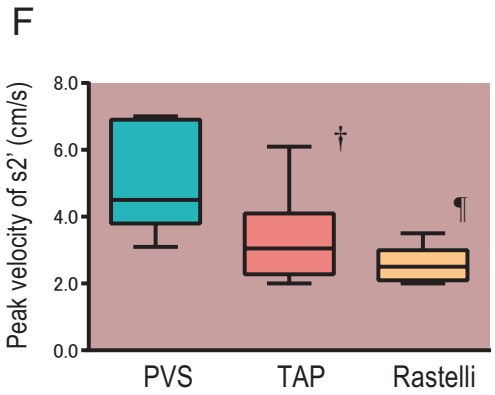
F
Peak velocity of s2' (cm/s)
8.0
6.0
4.0
2.0
0.0
†
¶
PVS
TAP
Rastelli

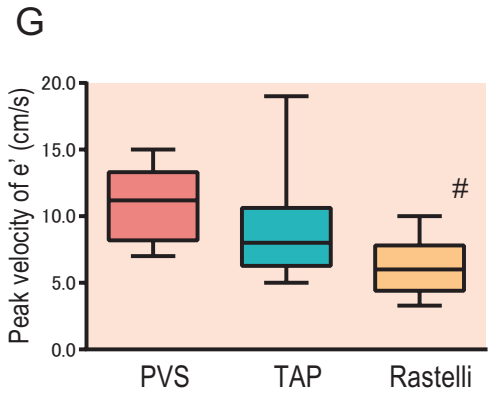
G
Peak velocity of e' (cm/s)
20.0
15.0
10.0
5.0
0.0
#
PVS
TAP
Rastelli

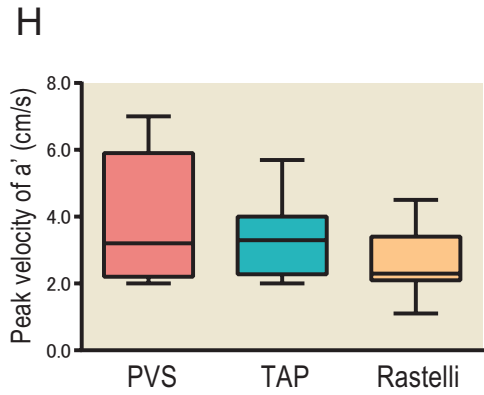
H
Peak velocity of a' (cm/s)
8.0
6.0
4.0
2.0
0.0
PVS
TAP
Rastelli

Figure 3

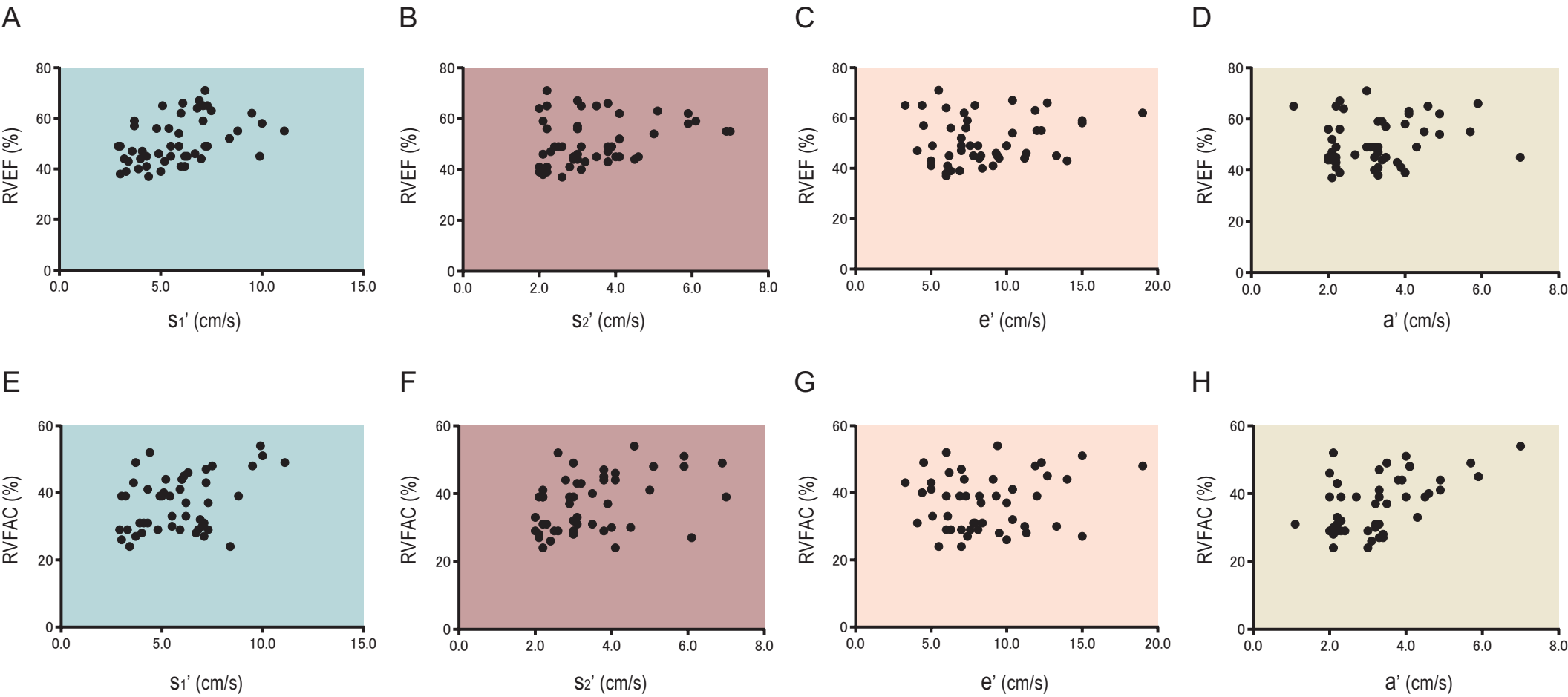
A
B
C
D
E
F
G
H
RVEF (%)
RVFAC (%)
s1' (cm/s)
s2' (cm/s)
e' (cm/s)
a' (cm/s)
0
20
40
60
80
0.0
2.0
4.0
5.0
6.0
10.0
15.0
20.0

Figure 4

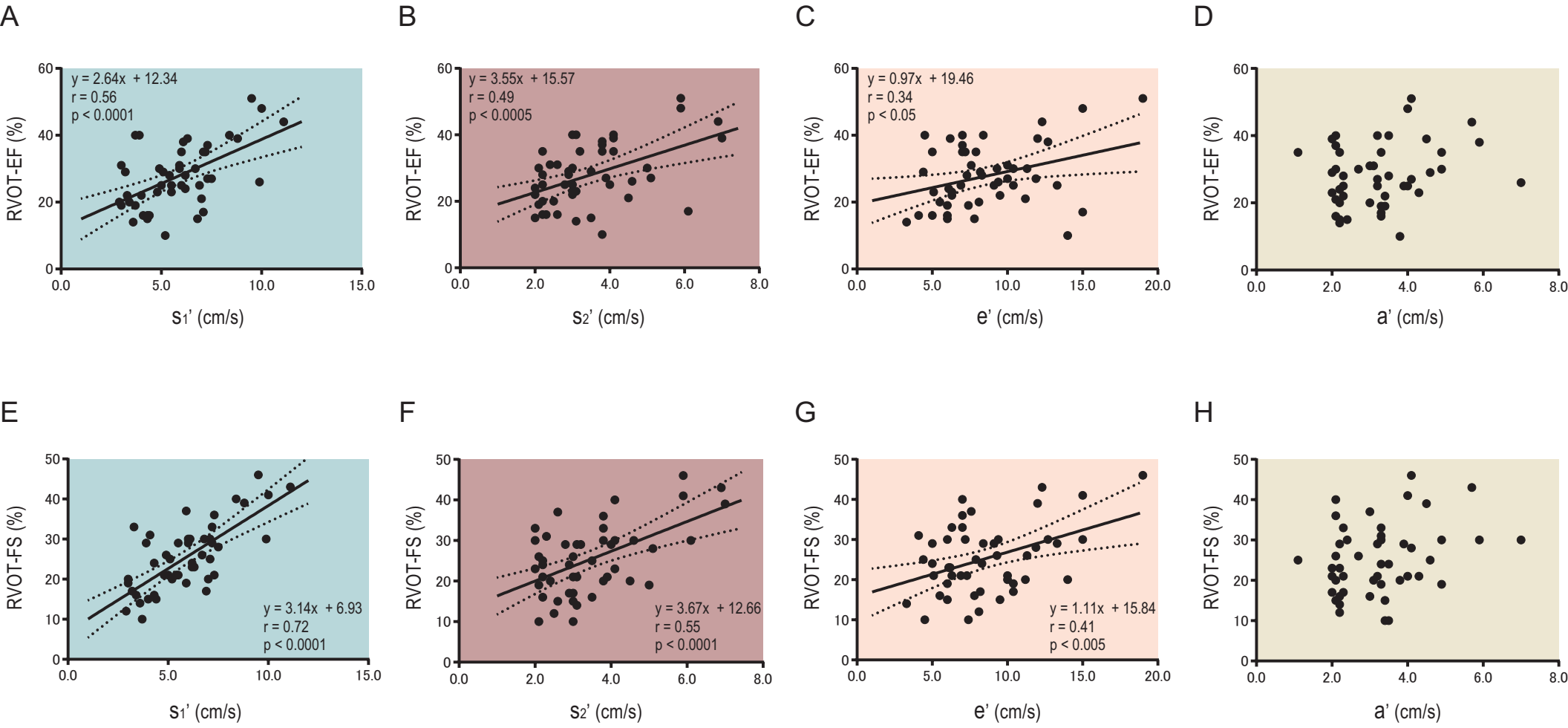
A
y = 2.64x + 12.34
r = 0.56
p < 0.0001
RVOT-EF (%)
s1' (cm/s)
B
y = 3.55x + 15.57
r = 0.49
p < 0.0005
RVOT-EF (%)
s2' (cm/s)
C
y = 0.97x + 19.46
r = 0.34
p < 0.05
RVOT-EF (%)
e' (cm/s)
D
RVOT-EF (%)
a' (cm/s)
E
y = 3.14x + 6.93
r = 0.72
p < 0.0001
RVOT-FS (%)
s1' (cm/s)
F
y = 3.67x + 12.66
r = 0.55
p < 0.0001
RVOT-FS (%)
s2' (cm/s)
G
y = 1.11x + 15.84
r = 0.41
p < 0.005
RVOT-FS (%)
e' (cm/s)
H
RVOT-FS (%)
a' (cm/s)

Figure 5

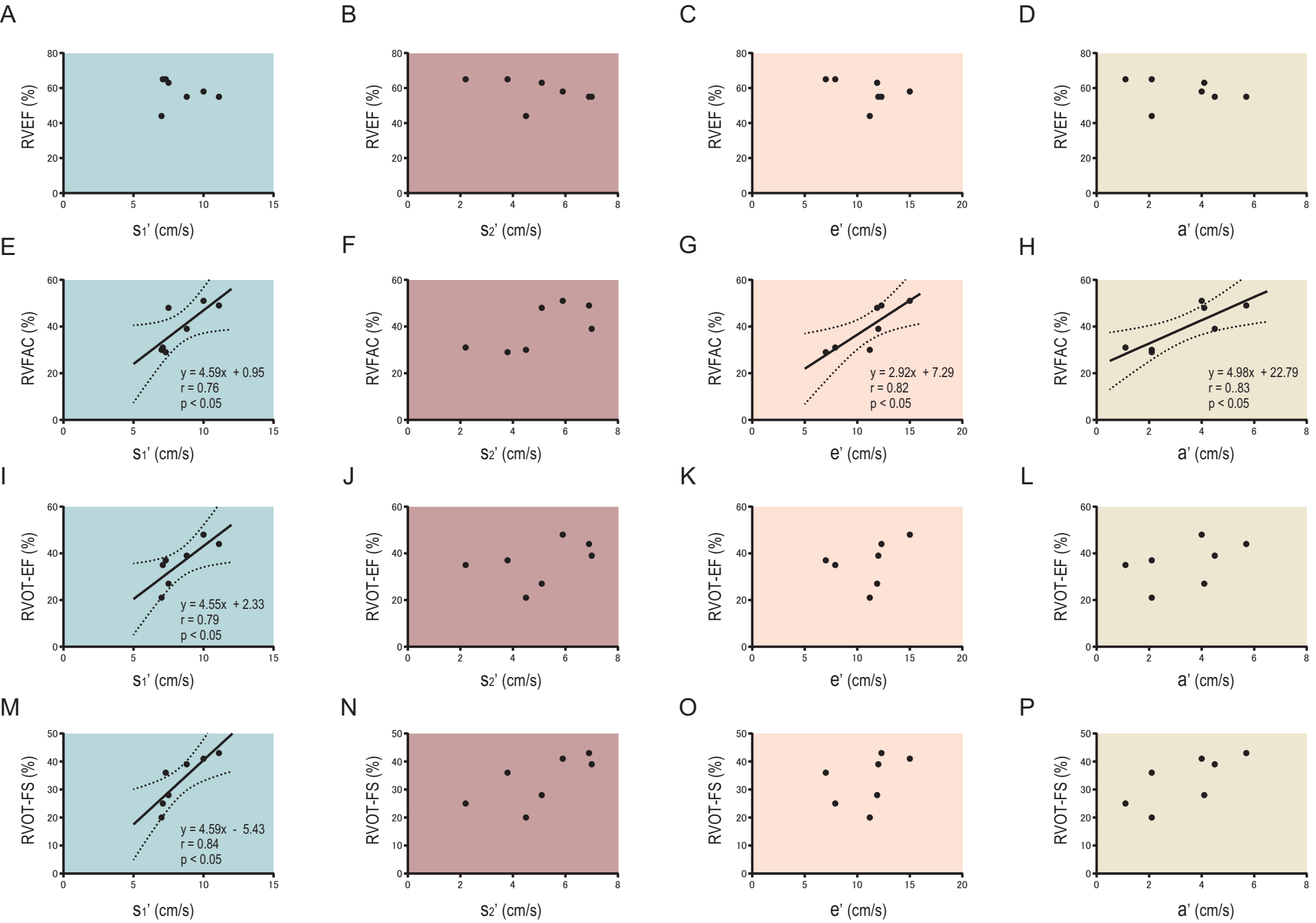
A
B
C
D
E
F
G
H
I
J
K
L
M
N
O
P
RVEF (%)
RVFAC (%)
RVOT-EF (%)
RVOT-FS (%)
s1' (cm/s)
s2' (cm/s)
e' (cm/s)
a' (cm/s)
y = 4.59x + 0.95
r = 0.76
p < 0.05
y = 2.92x + 7.29
r = 0.82
p < 0.05
y = 4.98x + 22.79
r = 0..83
p < 0.05
y = 4.55x + 2.33
r = 0.79
p < 0.05
y = 4.59x - 5.43
r = 0.84
p < 0.05

Figure 6

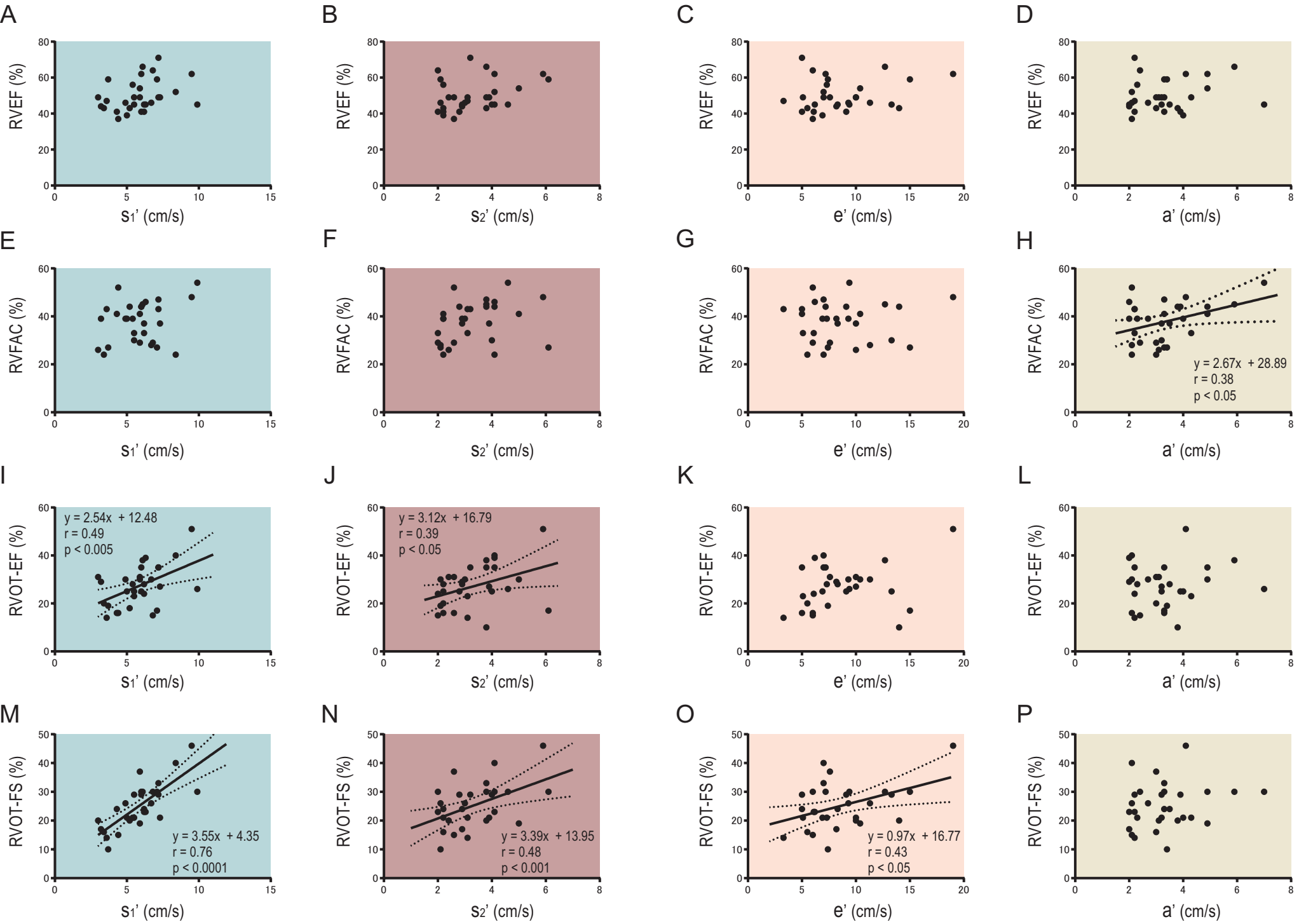
A
RVEF (%)
S1' (cm/s)
B
RVEF (%)
S2' (cm/s)
C
RVEF (%)
e' (cm/s)
D
RVEF (%)
a' (cm/s)
E
RVFAC (%)
S1' (cm/s)
F
RVFAC (%)
S2' (cm/s)
G
RVFAC (%)
e' (cm/s)
H
RVFAC (%)
y = 2.67x + 28.89
r = 0.38
p < 0.05
a' (cm/s)
I
RVOT-EF (%)
y = 2.54x + 12.48
r = 0.49
p < 0.005
S1' (cm/s)
J
RVOT-EF (%)
y = 3.12x + 16.79
r = 0.39
p < 0.05
S2' (cm/s)
K
RVOT-EF (%)
e' (cm/s)
L
RVOT-EF (%)
a' (cm/s)
M
RVOT-FS (%)
y = 3.55x + 4.35
r = 0.76
p < 0.0001
S1' (cm/s)
N
RVOT-FS (%)
y = 3.39x + 13.95
r = 0.48
p < 0.001
S2' (cm/s)
O
RVOT-FS (%)
y = 0.97x + 16.77
r = 0.43
p < 0.05
e' (cm/s)
P
RVOT-FS (%)
a' (cm/s)

Figure 7

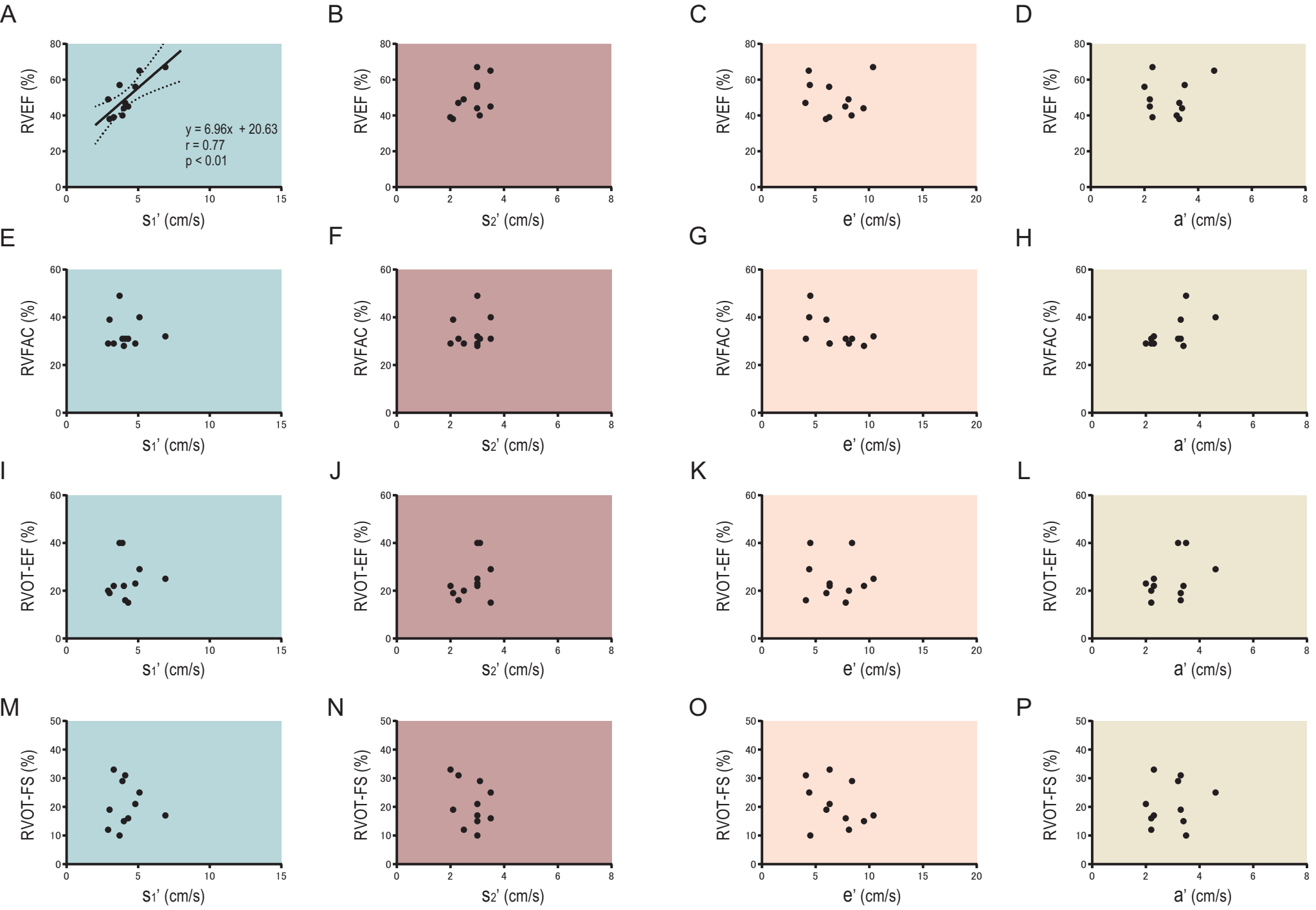
A
B
C
D
E
F
G
H
I
J
K
L
M
N
O
P
RVEF (%)
RVFAC (%)
RVOT-EF (%)
RVOT-FS (%)
S1' (cm/s)
S2' (cm/s)
e' (cm/s)
a' (cm/s)
y = 6.96x + 20.63
r = 0.77
p < 0.01

Figure 8

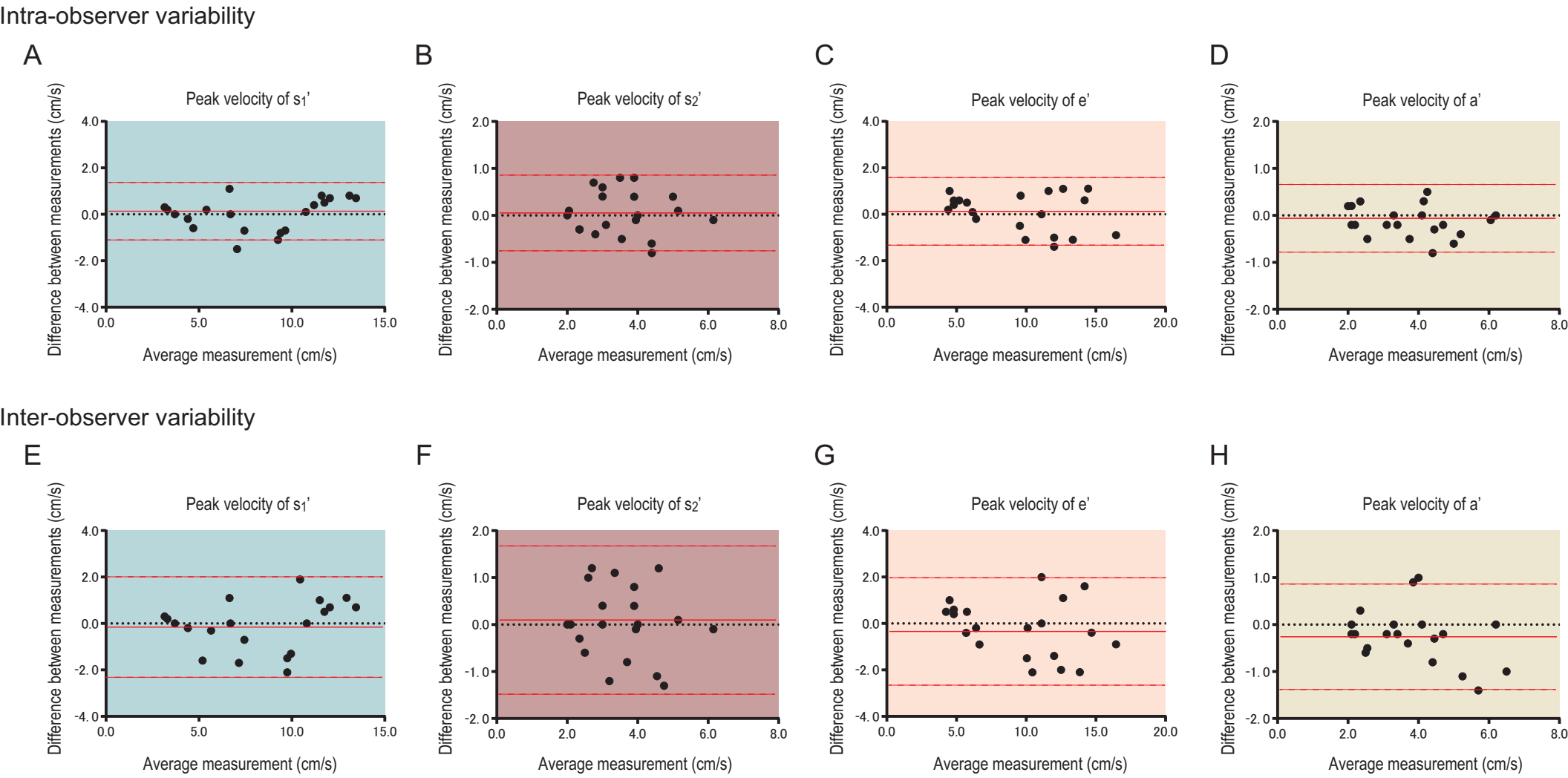
Intra-observer variability
A
Peak velocity of s1'
B
Peak velocity of s2'
C
Peak velocity of e'
D
Peak velocity of a'
Inter-observer variability
E
Peak velocity of s1'
F
Peak velocity of s2'
G
Peak velocity of e'
H
Peak velocity of a'
Difference between measurements (cm/s)
Average measurement (cm/s)